

# Toward a Global Model of Methylmercury Biomagnification in Marine Food Webs: Trophic Dynamics and Implications for Human Exposure

Peipei Wu and Yanxu Zhang\*



Cite This: <https://doi.org/10.1021/acs.est.3c01299>



Read Online

ACCESS |

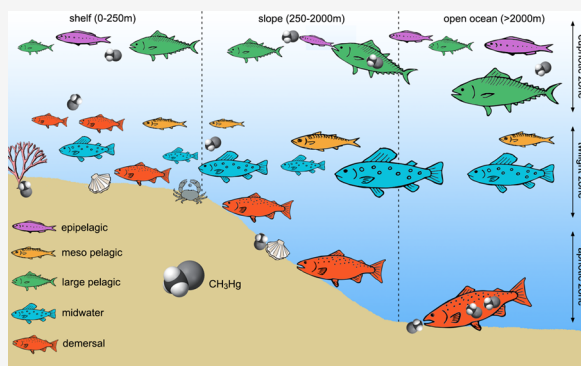
Metrics & More

Article Recommendations

Supporting Information

**ABSTRACT:** Marine fish is an excellent source of nutrition but also contributes the most to human exposure to methylmercury (MMHg), a neurotoxicant that poses significant risks to human health on a global scale and is regulated by the Minamata Convention. To better predict human exposure to MMHg, it is important to understand the trophic transfer of MMHg in the global marine food webs, which remains largely unknown, especially in the upper trophic level (TL) biota that is more directly relevant to human exposure. In this study, we couple a fish ecological model and an ocean methylmercury model to explore the influencing factors and mechanisms of MMHg transfer in marine fish food webs. Our results show that available MMHg in the zooplankton strongly determines the MMHg in fish. Medium-sized fish are critical intermediaries that transfer more than 70% of the MMHg circulating in food webs. Grazing is the main factor to control MMHg concentrations in different size categories of fish. Feeding interactions affected by ecosystem structures determine the degree of MMHg biomagnification. We estimate a total of 6.1 metric tons of MMHg potentially digested by the global population per year through marine fish consumption. The model provides a useful tool to quantify human exposure to MMHg through marine fish consumption and thus fills a critical gap in the effectiveness evaluation of the convention.

**KEYWORDS:** methylmercury, biomagnification, food webs, feeding interactions, human exposure, MITgcm, FEISTY



## 1. INTRODUCTION

Methylmercury ( $\text{CH}_3\text{Hg}^+$  or MMHg) is a neurotoxicant linked to neurocognitive defects in fetuses and cardiovascular diseases in adults.<sup>1–3</sup> The global health impacts resulting from MMHg exposure are estimated to cost 117 billion U.S. dollars per year.<sup>4</sup> Seafood consumption is the main route of human exposure to MMHg,<sup>4–6</sup> of which the MMHg content is influenced by ocean MMHg levels and their trophic dynamics.<sup>7–9</sup> Seafood is a good source of high-quality proteins, vitamins, minerals, or polyunsaturated fatty acids.<sup>10</sup> Therefore, reducing the MMHg content in fish rather than seafood consumption is a preferred policy position. The Minamata Convention, an internationally legally binding treaty that aims to reduce mercury emissions, came into effect in 2017 and seeks to reduce exposure to MMHg. As part of the convention, countries will monitor the MMHg levels in human-consumed biota (<https://www.mercuryconvention.org>). The underlying expectation of this agreement is that reductions in emissions of mercury will result in reductions of MMHg in seafood.

MMHg levels are highly variable in different marine food webs across the global ocean.<sup>11,12</sup> The first step of MMHg into food webs is the uptake by plankton, which determines MMHg in top-level organisms.<sup>13</sup> When transferred to fish, MMHg

concentration is elevated as fish ages and is increased by two to three times with each trophic level (TL), which is known as biomagnification.<sup>14</sup> As a result, MMHg content is the greatest in the old and large fish at the top of food chains.<sup>15</sup> Observations also show that higher water temperature can stimulate growth thus decreasing the MMHg concentration in the biota (i.e., growth dilution)<sup>16</sup> and increase the excretion rates of MMHg,<sup>17</sup> evidenced by the phenomenon that biomagnification is positively related to latitude.<sup>18</sup> The lower biomagnification at low latitudes is also attributed to the higher diversity and more complex food webs there.<sup>19</sup> High primary productivity reduces the MMHg biomagnification as high-quality food stimulates growth and lowers ingestion rates, reducing the accumulation and trophic transfer of MMHg.<sup>18,20</sup> A simulation study also suggests that MMHg biomagnification

**Received:** February 16, 2023

**Revised:** April 1, 2023

**Accepted:** April 3, 2023

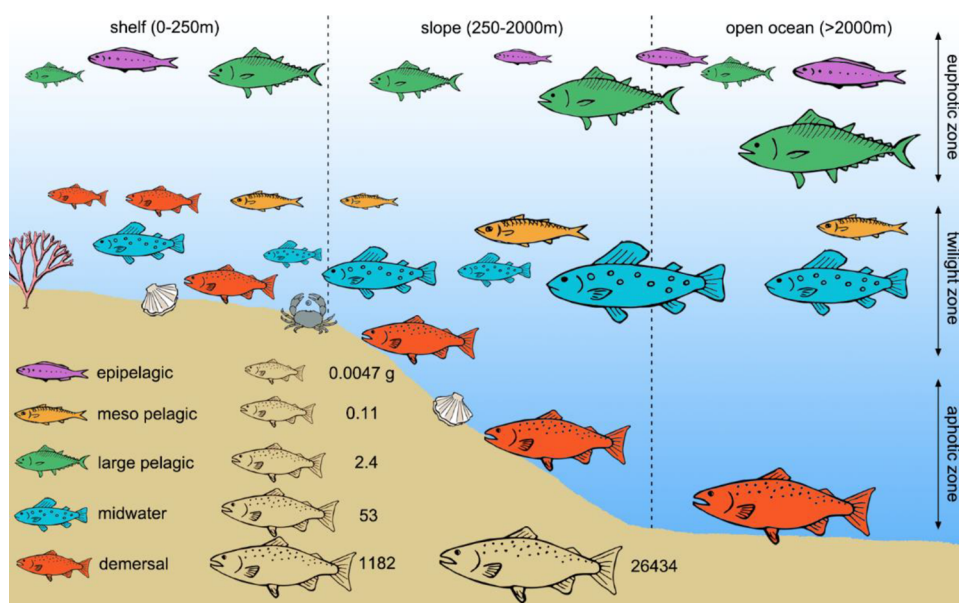


**Figure 1.** Illustration of the simplified marine fish community: fish guilds and vertical distribution. The shapes and colors indicate the fish guild. The sizes indicate the central weight of an individual fish (g wet weight) in each size group, following the FEISTY model. Note that the location of each size group does not necessarily indicate the horizontal position of that group. The horizontal distribution of each size group is shown in Figure S2.

is the highest in oligotrophic systems due to the high trophic transfer of MMHg.<sup>21</sup>

How MMHg transfers from planktonic food webs to upper TL biota on a global scale is still largely unknown, especially how this further influences human exposure to MMHg. This greatly hinders our ability to predict the potential response of human-consumed biota to anthropogenic emission reductions proposed by the Minamata Convention. Measurements are also sparse and limited to the coastal ocean ecosystems.<sup>18</sup> The existing global simulations only contain the low TLs (phytoplankton and zooplankton).<sup>21</sup> In this study, we develop a global model that extends the food web dynamics to higher TLs. The model couples an ocean methylmercury model<sup>8,21,22</sup> to a state-of-the-art fish ecological model with diverse fish sizes and function groups.<sup>23,24</sup> There are five fish guilds in the fish model: epipelagic, mesopelagic, large pelagic, mid-water predators, and demersal fish. Fish with different body sizes have variable vertical distributions and feeding strategies. The model output is evaluated against existing empirical data. We explore the relationship between trophic dynamics and MMHg biomagnification. We also use a fisheries catch database to estimate the potential human exposure to MMHg through marine fish consumption.<sup>25</sup>

## 2. METHODS

**2.1. General Description.** The coupled model consists of a global marine fish ecological model (FishErIes Size and functional TYPe model, FEISTY) and a methylmercury transport and transformation model (MITgcm). They have a resolution of 1° spatially across the global ocean. The fish biomass, grazing fluxes, mortality fluxes, growing fluxes, and reproduction fluxes from the FEISTY model serve as inputs for the methylmercury model. These variables vary across the global ocean depending on the structures of fish food webs (e.g., the prey–predator relationships) and the environmental factors (e.g., water temperature). The MMHg concentrations of seawater and zooplankton that drive the marine fish food

webs are taken from the previous modeling and field studies,<sup>8,26–29</sup> while the MMHg concentrations of fish are simulated in the coupled model. The details of the two models are elaborated below.

**2.2. Fish Model.** The fish model is in a size- and trait-based modeling framework (FEISTY).<sup>23,24</sup> It comprises five fish guilds: epipelagic fish, mesopelagic fish, large pelagic fish, mid-water predators, and demersal fish. Differences among fish guilds are distinguished by maximum body weight and vertical habitat strategies. Epipelagic fish and mesopelagic fish (each guild has four size groups) have smaller maximum weight than the other three (each guild has six size groups) (Figure 1). The two largest size groups in each guild, i.e., the mature fish, allocate energy to the smallest size group as reproduction. Fish in one size group will be counted as the next larger size group when growing up.

The vertical distribution of fish varies by the guilds and size groups (Figure 1). The feeding interactions rely on habitat overlap in the water column and the rule that large predators eat smaller preys.<sup>30</sup> Epipelagic fish live in the upper water and primarily feed on zooplankton. Mesopelagic fish are used to living in a twilight environment and have diel vertical migration: being at depth during the day and at the surface during the night. Large pelagic fish are the most abundant at the surface, feeding on plankton in earlier life stages and grazing on fish later in life. They also travel to the twilight zone to prey on mesopelagic fish during the daytime. Juvenile mid-water predators live in the twilight zone during the daytime and move to the surface at night while the adult live in the twilight zone the whole day. The early juvenile mid-water predators feed on zooplankton, and the older ones tend to graze on fish. Different from the above fish guilds that primarily depend on pelagic energy pathways, demersal fish rely on both pelagic and benthic energy pathways.<sup>23</sup> Demersal fish are mainly located in the coastal oceans where primary production is high enough to support large fishery catches that account for 50% of global marine catch.<sup>31–33</sup> Early juvenile demersal fish

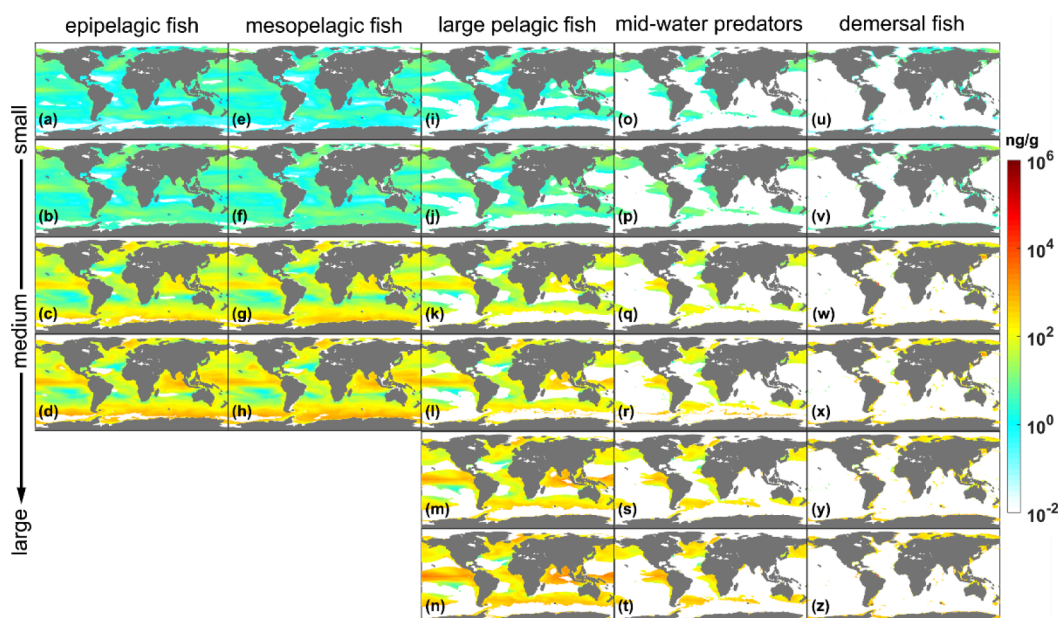


**Figure 2.** Simulated spatial pattern of MMHg concentrations in marine fish in the global ocean [ng/g wet weight]. (a–d) Epipelagic fish, (e–h) mesopelagic fish, (i–n) large pelagic fish, (o–t) mid-water predators, and (u–z) demersal fish. The arrow indicates an increase in fish body sizes.

feed in the upper water while late juvenile feed at the bottom, and they mainly live on benthonic production. Adult demersal fish live between the surface and the bottom and feed on fish.

**2.3. Methylmercury Model.** The methylmercury model is based on Zhang et al. and Wu et al.,<sup>8,21,22,34</sup> which simulates the transport and biogeochemical cycle of marine methylmercury (Tables S1 and S3). Fish get MMHg from seawater and food that are namely small to medium-sized (0.2–2 mm) and large zooplankton (2–20 mm), benthic production, and other fish with smaller body size. They lose MMHg by excretion and mortality. The mature groups of each fish guild transfer MMHg to larval fish (the smallest size group) during reproduction. As fish grow, they move into larger size groups, together with MMHg in their body.

MMHg flux into ( $\text{Flux}_{\text{in}}$ ) size groups other than the smallest one is:

$$\text{Flux}_{\text{in}} = k_{\text{BC}} \times \text{MMHg}_{\text{sea}} + k_{\text{GZ}} \times \text{AE}_{\text{MMHg}} \times \text{MMHg}_{\text{prey}} + k_{\text{GR}} \times \text{MMHg}_{\text{smaller}} \quad (1)$$

where  $k_{\text{BC}}$ ,  $k_{\text{GZ}}$ , and  $\text{AE}_{\text{MMHg}}$  are the bioconcentration rate, grazing rate, and MMHg assimilation efficiency of this size group, respectively.  $k_{\text{GR}}$  is the growth rate from the next smaller size group.  $\text{MMHg}_{\text{sea}}$  is the MMHg concentrations of seawater.  $\text{MMHg}_{\text{prey}}$  is the MMHg concentrations of this group's prey, including both zooplankton and fish that have smaller sizes and overlapping habitats.  $\text{MMHg}_{\text{smaller}}$  is the MMHg concentrations of the next smaller size group that will grow into this size group.

MMHg flux into ( $\text{Flux}_{\text{in}}$ ) the smallest size group is:

$$\text{Flux}_{\text{in}} = k_{\text{BC}} \times \text{MMHg}_{\text{sea}} + k_{\text{GZ}} \times \text{AE}_{\text{MMHg}} \times \text{MMHg}_{\text{prey}} + k_{\text{PD}} \times \text{MMHg}_{\text{prod}} \times \text{TE}_{\text{MMHg}} \quad (2)$$

where  $k_{\text{PD}}$  and  $\text{TE}_{\text{MMHg}}$  are the reproducing rate and the MMHg transfer efficiency through reproduction, respectively.

$\text{MMHg}_{\text{prod}}$  is the MMHg concentrations of the mature fish that can reproduce (the two largest size groups of each fish guild).

MMHg flux out of ( $\text{Flux}_{\text{out}}$ ) size groups is:

$$\text{Flux}_{\text{out}} = \begin{cases} (k_{\text{MT}} + k_{\text{EX}} + k_{\text{GZ}} + k_{\text{PD}}) \times \text{MMHg}_{\text{fish}} \\ (k_{\text{MT}} + k_{\text{EX}} + k_{\text{GR}} + k_{\text{GZ}} + k_{\text{PD}}) \times \text{MMHg}_{\text{fish}} \\ (k_{\text{MT}} + k_{\text{EX}} + k_{\text{GR}} + k_{\text{GZ}}) \times \text{MMHg}_{\text{fish}} \end{cases}$$

the largest size group  
the second largest size group  
other size groups

(3)

where  $k_{\text{MT}}$  and  $k_{\text{EX}}$  are the mortality rate and excretion rate of this size group, respectively.  $k_{\text{GR}}$  is the growing rate from this size group to the next larger size group.  $k_{\text{GZ}}$  is the grazing rate of this group's predators.  $k_{\text{PD}}$  is the reproducing rate of this size group.  $\text{MMHg}_{\text{fish}}$  is the MMHg concentrations of this size group (more details in Table S2).

**2.4. TL and Trophic Magnification Factor (TMF).** TL indicates the position of an organism in the food chain. The TL of marine fish is defined as:<sup>35</sup>

$$\text{TL}_i = 1 + \sum_j (\text{TL}_j \cdot \text{DC}_{i,j}) \quad (4)$$

where  $\text{TL}_i$  is the TL of predator  $i$ ,  $\text{TL}_j$  is the TL of prey  $j$  of predator  $i$ , and  $\text{DC}_{i,j}$  is the fraction of prey  $j$  in the diet of predator  $i$ .

The relationship between the base-10 logarithm of MMHg concentration and TLs is defined as:<sup>18,36</sup>

$$\text{Log}_{10}[\text{MMHg}] = b\text{TL} + a \quad (5)$$

where  $a$  is the intercept and  $b$  is the slope of the relationship, which varies with space and time. The TMF is defined as:<sup>36</sup>

$$\text{TMF} = 10^b \quad (6)$$

**2.5. Fish and MMHg Catch.** We use the global marine fisheries catch data in the year 2014 from Watson.<sup>25</sup> The data set is a map of catch rates (metric tons per square km of ocean) for each spatial cell separated by fishing country and fish taxa. The FEISTY model focuses on marine fish, so we only analyze the catch data of marine fish. Other sea life, such as mammals, invertebrates, and reptiles, are not considered in this study. The TL, length, and habitat information of fish taxa are from the Fishbase Database (<https://www.fishbase.org>). This information is used to allocate a fish taxon to one of the 26 fish groups in the FEISTY model to obtain their MMHg concentrations. More specifically, a fish taxon is matched to one of the five fish guilds in the FEISTY model based on its name and habitat. Then it is matched to one size group of this fish guild based on its TL and length. According to the location of fishing, i.e., the latitude and longitude, we can obtain the MMHg concentration of the simulated fish that is corresponding to this fish taxon, which is used as the MMHg concentration of this fish taxon. If the modeled fish group is absent in one spatial cell, the fish catch is not considered. Using the fish taxa and catch rate of a country, combined with the simulated MMHg concentrations in fish mentioned above, we can also calculate the MMHg catch of this country.

### 3. RESULTS AND DISCUSSION

**3.1. MMHg Contents in Fish.** The simulated global average MMHg concentrations of the 26 fish groups vary from 5.0 to 555 ng/g wet weight (Figure 2). Large fish have MMHg concentrations two orders of magnitude higher than small fish. The simulated MMHg concentration of total mature fish (the two largest groups of each fish guild that are more relevant to the fishery and human exposure) is  $209 \pm 958$  ng/g. Due to larger sizes, large pelagic fish and mid-water predators have higher simulated MMHg concentrations ( $250 \pm 481$  and  $199 \pm 143$  ng/g, respectively, Figure 2i–t) than epipelagic fish and mesopelagic fish ( $105 \pm 119$  and  $114 \pm 127$  ng/g, respectively, Figure 2a–h). The simulated MMHg concentration in demersal fish is the highest ( $430 \pm 3258$  ng/g) as they feed on benthic production in the coastal oceans where the high river export of Hg causes large sedimentation flux of MMHg.<sup>37</sup> Measurements in many oceans also show that MMHg content in fish is increased with the depth of their occurrence. In other words, MMHg concentrations in demersal fish are higher than those in pelagic fish because the MMHg in the water column is increased with depth.<sup>38–42</sup>

The simulated MMHg concentrations in fish also increase with the TLs that can be diagnosed by the food composition (Figure 3). That is, the larger or older fish (both have higher TLs) have higher MMHg concentrations than the smaller or younger ones. The modeled average MMHg concentration in fish is 115 ng/g for TLs <3.5, 199 ng/g for TLs 3.5–4, and 348 ng/g for TLs > 4. This trend is consistent with the observations for these three TL ranges: 106, 267, and 434 ng/g, respectively (Supplementary Materials). The model also captures the latitudinal pattern in fish MMHg concentrations, which are lower at subtropics (20–30° in both hemispheres) because of the extremely low seawater and zooplankton MMHg levels in the open ocean gyres. The observations are slightly higher in these latitude ranges because the sampling sites are mostly located in coastal oceans. Fish MMHg levels are higher in equatorial and high latitudes (>60° in both hemispheres), reflecting the high MMHg levels of zooplankton (Figure S1a). Overall, this indicates that available MMHg from

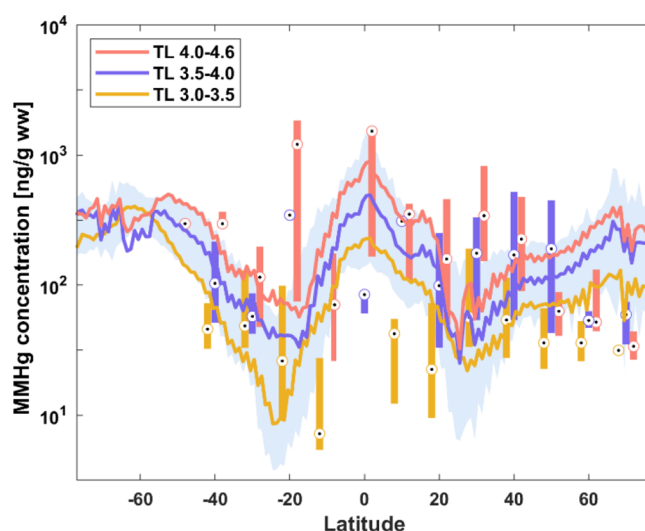


**Figure 3.** Latitudinal variation of MMHg concentrations in marine fish of different trophic levels. The curves are the simulated values, while the vertical bars are the observed values with the circle as the median and the upper and lower edges as the upper and lower quartiles, respectively (see Supplementary Materials for more details of observed values).

primary consumers (e.g., zooplankton) at the base of food webs, whose MMHg content is primarily affected by the MMHg bioconcentration of phytoplankton from seawater,<sup>8</sup> can largely control the MMHg in higher trophic predators like fish.<sup>13</sup>

**3.2. MMHg Trophic Transfer.** The trophic dynamics of MMHg suggest that food is the primary source of MMHg for fish, while the intake from seawater accounts for only less than 0.1% of the obtained MMHg. For the smallest size fish groups, the maternal transfer of MMHg from mature fish plays a slightly larger role (~1.4%) and this fraction is even larger for the juvenile demersal fish (8.6%). On the other hand, the largest loss term for the MMHg in fish is by being preyed on, followed by excretion and mortality (Figure 4a,d).

Zooplankton and benthic production fuel initially the MMHg transfer to the upper TLs through diet (Figures 4a and S4).<sup>9,13</sup> Globally, large zooplankton and benthic production supply  $4633$  and  $589$  kmol yr<sup>-1</sup> of MMHg to pelagic fish and demersal fish, respectively. Whether zooplankton or benthic taxa contribute more varies geographically depending on their MMHg concentrations.<sup>9,43</sup> After entering the fish food webs, the medium-sized fish (e.g., the largest epipelagic and mesopelagic fish) are the most critical intermediaries in transferring MMHg to higher TLs (Figure 4a). They digest  $5586$  kmol yr<sup>-1</sup> of MMHg from their prey, accounting for 71% of the total MMHg intake by fish from food (Figure 4b), and transfer  $2397$  kmol yr<sup>-1</sup> of MMHg to the higher TLs, representing 84% of the total MMHg transferred by fish to their predators (Figure 4a), higher than their biomass in proportion to the total one (~50%).

MMHg transferred during growth is much less than that by grazing. More predation compensates for the possible decline in MMHg concentrations due to growth (Figure 4b,c). Also, growth dilution of MMHg may vary across ontogenetic life stages of fish, and it is still unknown.<sup>43</sup> Our model simulates the fish growth with an Euler perspective, i.e., we discuss the growth of whole fish groups rather than individual fish and the transferred MMHg is counted as a fish group grows to an

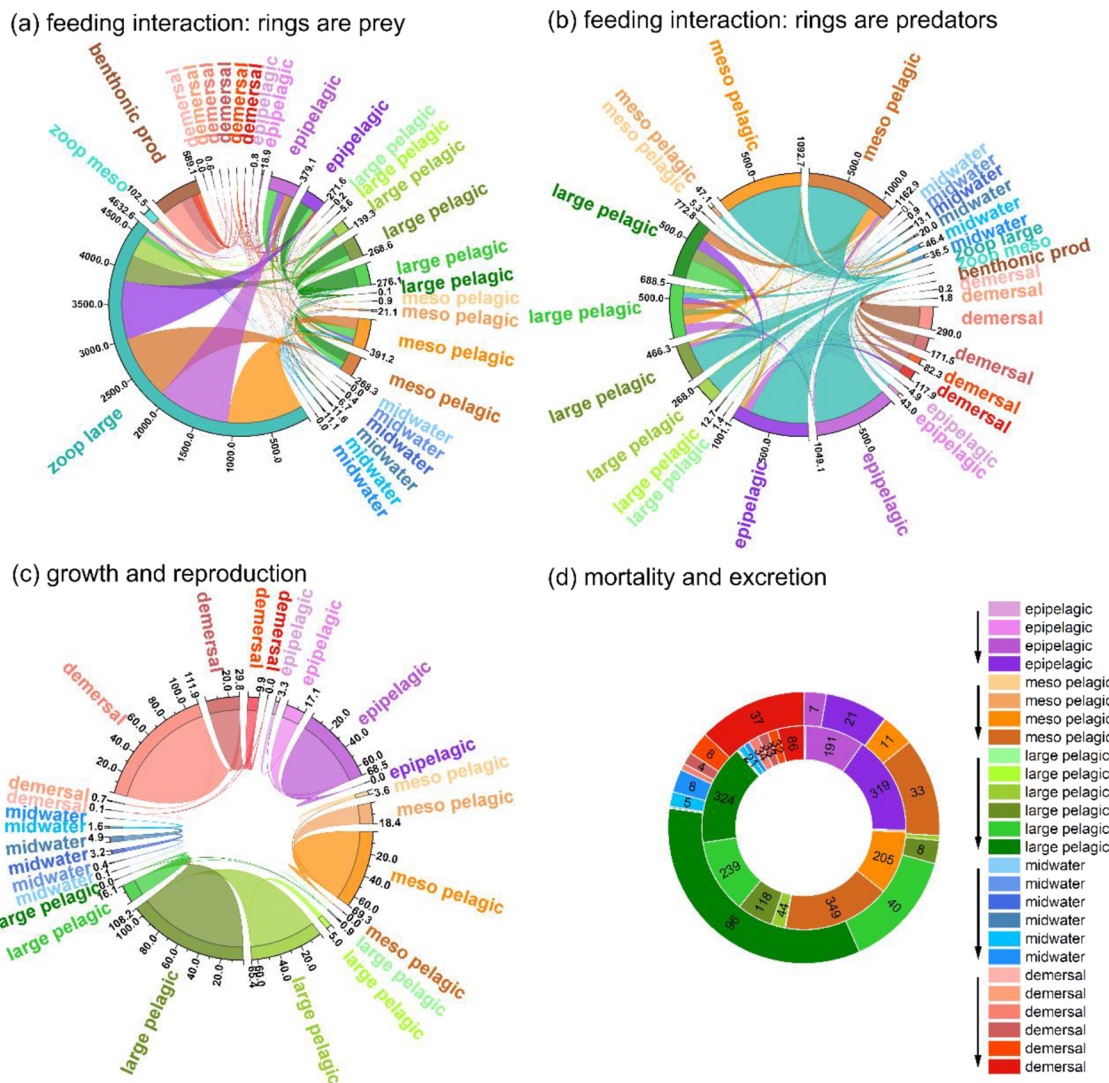


**Figure 4.** Trophic dynamics of MMHg in the global ocean. (a, b) Feeding interactions. The color of the outer circular rings and the linkers indicates the type of biota, i.e., zooplankton or fish groups. The linkers represent graze fluxes between the connected predators and prey with the numbers next to the rings as the magnitudes of grazing fluxes [ $\text{kmol yr}^{-1}$ ]. Panels a and b show the fluxes from a prey or predator’s viewpoint, respectively. In panel (a), the width of the rings shows the MMHg fluxes that are being preyed. The color of the linkers indicates the predators, and the width of the linkers represents the fraction of grazing fluxes by corresponding predators. In panel (b), the width of the rings shows the total MMHg fluxes into each group. The color of the linkers indicates the prey, and the width of the linkers represents the contributions of corresponding prey. (c) Reproducing and growing fluxes [ $\text{kmol yr}^{-1}$ ]. The linkers between the mature fish group (i.e., the two largest size groups of each fish guild) and the smallest size group show the MMHg transfer fluxes via reproducing. The remaining linkers show the growing fluxes. (d) Mortality fluxes (outer rings) and excretion fluxes (inner rings) of MMHg [ $\text{kmol yr}^{-1}$ ]. The arrows indicate an increase in body sizes of each fish guild.

immediate bigger-size one. The model simulates that the MMHg transferred by medium-sized fish during growth is the most important. Despite the higher biomass of large size groups, they transfer much less MMHg to the largest fish during growth than the medium-sized groups (Figure 4c). This indicates that growth plays a small role on the MMHg accumulation of fish in our simulation at a fish group level, especially for the large fish group. The growth rate varies significantly among fish species and contributes differently to MMHg content in fish. Some field studies found that the growth rate primarily regulates the MMHg concentrations in individual fish samples,<sup>16,44</sup> while some studies found that differences of MMHg content are not related to the growth rate.<sup>45,46</sup> Although the smaller medium-sized fish lose the largest amount of MMHg during growth, they have higher

MMHg concentrations than the fish at lower TLs (Figure 2). Their age and trophic position allow them to accumulate abundant MMHg from food that overweighs growth dilution.

**3.3. MMHg Biomagnification.** The trophic magnification factors (TMFs) of MMHg are spatially variable across the global ocean (Figure 5). As most of the observations were conducted in the coastal oceans, we limit the comparison with the model along the coasts. Our model is not well suited for coastal simulations because of the relatively coarse resolution, but the modeled TMF [2.8 (1.9–5.0 as 1.5 times IQR)] is close to the observations [1.4 (0.16–14)]. The modeled TMF range is narrower than the observed one, largely due to the highly simplified simulated ecosystem and food web structures. Some trophic positions are absent in the model, which results in fewer variations of TMF. Also, some TMFs are calculated

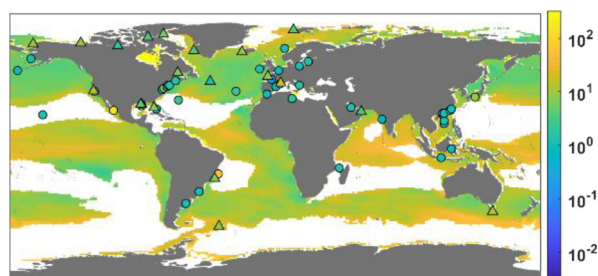


**Figure 5.** Trophic magnitude factors (TMF) of MMHg in fish food webs in the global ocean. Triangle markers show the TMFs obtained directly from previous studies, and the circle markers show the TMFs calculated using the observed MMHg concentrations shown in Figure 3. Due to the extremely scarce fish biomass and short food-chain length (Figures S2 and S3), TMFs are not shown in the subtropical gyres and the Southern Ocean adjacent to the Antarctic continent.

based on the measured MMHg concentrations from different studies shown in Figure 3. Although the study areas of these studies are in the same model grid, the sampling time and sites are not necessarily consistent, neither be the structures of food webs. These inconsistencies in measurements may lead to less accurate observed TMFs. The model also simulates that TMFs along the coast, especially those in the highly productive areas (e.g., the coastal upwelling areas on the eastern edges of the Pacific and the Atlantic), are lower than TMFs in the open ocean (Figure 5). In the equatorial western Pacific and Atlantic and the areas between the ultra-oligotrophic subtropical gyres and highly productive waters, where TMFs are the highest, the primary production is generally low but can still support some fish at high TLs.<sup>47</sup> This is consistent with the previous model studies focusing on the marine plankton ecosystems.<sup>21,22</sup> A meta-analysis of the observations also suggests the same phenomenon that TMFs are negatively correlated with productivity.<sup>18</sup>

Typical food web structures in different ocean environments reflect different MMHg feeding interactions (Figure 6). In nearshore areas, e.g., continental slopes and shelf systems (Figure 6b,c), TMFs are low and food webs are highly complex as fish have abundant food sources. Demersal fish, which have the largest MMHg content, rely on both pelagic and benthic energy pathways depending on their life stages: the early juvenile/small feed on only zooplankton, the late juvenile/medium primarily on benthos and other fish, and the mature/large on other large pelagic and demersal fish. Consequently, demersal fish have a rich intake of MMHg at each life stage, and the MMHg content increases gently with increasing body size/TL. In eutrophic open oceans where TMFs are also low, food webs are a bit less complex than those in nearshore oceans as demersal fish are absent. In these regions, large predators are dominant and prey on a variety of fish (Figure 6a,f). In mesotrophic oceans where TMFs are relatively high, food webs are much less complex and epipelagic fish and mesopelagic fish are dominant (Figure 6d). These fish primarily graze on zooplankton with the mature occasionally eating the smaller fish. The absence of large-sized fish results in a narrow span of TLs, so changes in MMHg content of fish with TLs can lead to high slopes, i.e., high TMFs. In oligotrophic oceans, fish biomass is extremely scarce and only a few low-trophic-level fish exist (Figure 6e). Similar to the mesotrophic oceans, the TLs of fish have a relatively narrow span, resulting in very high TMFs of MMHg. The proportion

of predators at the highest TL is also higher despite the total low biomass.<sup>48,49</sup> Therefore, fish are subject to more intense grazing pressure, and relatively more MMHg is transferred through diet.<sup>21</sup> Overall, we found that the differences in the trophic structures, which is largely influenced by coastal proximity, ocean bathymetry, and primary production,<sup>50</sup> induce the variations in the TMFs across the global ocean.

**3.4. MMHg Catch.** We estimate that 6.1 Mg MMHg is contained in the global marine fish catch per year. Large pelagic and demersal fish are the two largest contributors to human MMHg exposure, accounting for 48 and 34%, respectively. The MMHg catch rate is the highest in the Northwest Pacific, the Northeast Atlantic, the Eastern Central Pacific, and the Indian Ocean (Figure 7a). The estimated MMHg catch is lower than that by Lavoie et al. (13 Mg yr<sup>-1</sup>)<sup>51</sup> as our model focuses on marine fish while Lavoie et al. considered all the fisheries catch, including fish, mammals, invertebrates, and reptiles. Indeed, the fish catch included in our study accounts for 26% of the total fisheries catch.

The spatial pattern of MMHg catch is partially decoupled with the fish catch (Figures 7a and S5a). In the Northwest Pacific and Northeast Atlantic, both the MMHg and fish catch are high. Indeed, the Northwest Pacific always exports the most MMHg via fisheries in the past several decades.<sup>51</sup> The Eastern Central Pacific and the Indian Ocean are also large contributors to MMHg catch despite the mild fish catch rate in these areas. Extremely high MMHg levels in fish compensate for the medium fish catch in these regions.

We calculate that Brazil has the largest amount of MMHg catch (1285 kg yr<sup>-1</sup>), accounting for 21% of the global total, followed by Indonesia (649 kg yr<sup>-1</sup>, 11%), China (509 kg yr<sup>-1</sup>, 8.4%), the USA (364 kg yr<sup>-1</sup>, 6.0%), Japan (289 kg yr<sup>-1</sup>, 4.8%), Russia (287 kg yr<sup>-1</sup>, 4.7%), the Republic of Korea (269 kg yr<sup>-1</sup>, 4.4%), Philippines (237 kg yr<sup>-1</sup>, 3.9%), Norway (223 kg yr<sup>-1</sup>, 3.7%), and Ecuador (158 kg yr<sup>-1</sup>, 2.6%) as the top 10 countries in MMHg catch (Figure 7). Among these countries, China (10% of the global fish catch), the USA (7.9%), Russia (7.9%), Indonesia (7.3%), Norway (6.2%), Japan (6.1%), and the Republic of Korea (2.8%) are in the top 10 list of fish catching countries (Figure S5).

MMHg catch of these countries has drastically different spatial and guild distributions (Figure 7b–g). Despite the largest MMHg catch, the fish catch of Brazil accounts for only 0.38% of the global total with 53% as demersal fish and 33% as large pelagic fish, primarily from the central and southwest Atlantic (Figures 7b and S5b). This is mainly caused by the very high MMHg concentrations of demersal fish in the central Atlantic near the mouth of the Amazon River (Figure 2). The largest Hg export from the Amazon River provides abundant substrate for methylation and subsequent bioaccumulation.<sup>37</sup> The observed MMHg concentrations in top predators in the Amazon River Basin and the Brazilian Equatorial Atlantic Ocean are among the highest globally,<sup>52–54</sup> which can be attributed to the feeding on deep water fish.<sup>54</sup> Fish caught by Indonesia are mainly from the western central Pacific and the eastern Indian Ocean (Figures 7c and S5c), with 49% as large pelagic guild. Similarly, 80 and 72% of the fish catch of the Philippines and Ecuador are large pelagic fish. Differently, 55% of the fish catch of China is epipelagic fish that has lower MMHg concentrations, with 29 and 16% as large pelagic and demersal fish, respectively. However, epipelagic fish are responsible for only 10% of MMHg catch of China, while

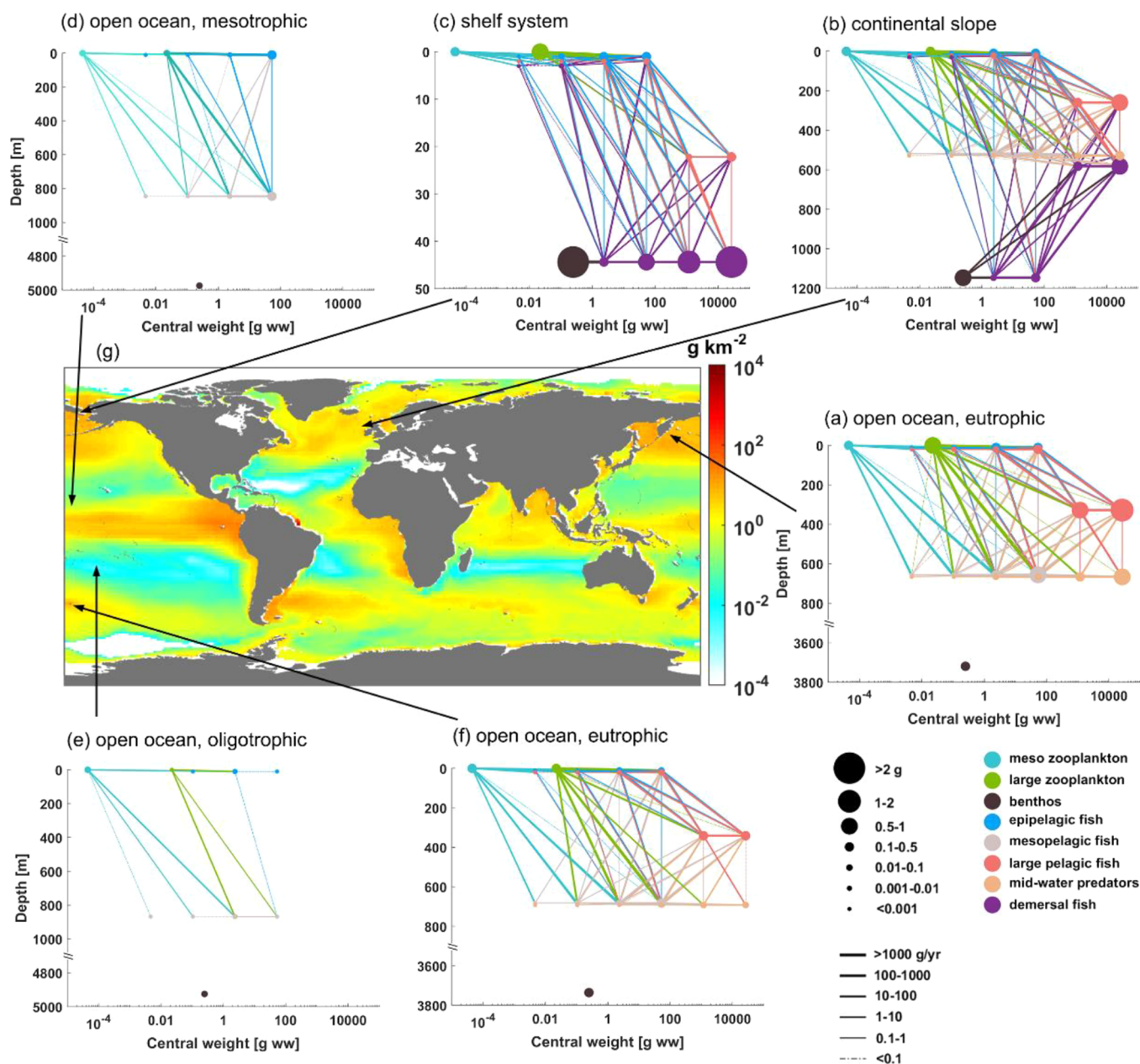


**Figure 6.** Food web structures in different ocean environments. The size of circles in panels (a–f) shows the amount of MMHg in fish per square kilometer [ $\text{g km}^{-2}$ ], and the thickness of lines shows the amount of MMHg transferred during feeding interactions per year per square kilometer [ $\text{g yr}^{-1} \text{km}^{-2}$ ]. The X-axis is the central weight of an individual fish in different fish groups, and the Y-axis is the ocean depth. Panel (g) shows the total amount of MMHg in all fish [ $\text{g km}^{-2}$ ].

large pelagic fish and demersal fish contribute 67 and 23%, respectively.

**3.5. Uncertainty.** Our model bears large uncertainties from the limitation in existing scientific knowledge and data. Due to the lack of available observed data, previous models that serve as the foundation of this study have their inherent uncertainties in simulating the MMHg concentrations of seawater, phytoplankton, zooplankton, and benthic production.<sup>8,21,22</sup> For example, the simulated average MMHg concentration of seawater is 38% lower than the measured one.<sup>8</sup> The deviation between the modeled MMHg concentrations and the observed ones is within an order of magnitude for different phytoplankton types.<sup>21</sup> High MMHg content in benthos in the Atlantic near Brazil is not well constrained by observations, resulting in large amounts of MMHg being transferred to

demersal fish and high MMHg catch of Brazil. However, the simulations in this study are overall comparable with much more fish MMHg measurements and capture the observed spatial trends (Figure 3). The model uncertainty of MMHg concentrations in fish is close to that in the phytoplankton, indicating that the uncertainty of previous models is not significantly amplified to higher TLs. The model is unable to simulate the specific fish species, and the classification of fish is highly simplified.<sup>23</sup> Sea life such as invertebrates, that contribute to human exposure, are excluded in the model.<sup>55</sup> These marine lives also indirectly affect human exposure by changing MMHg content in fish as they are important trophic links in food webs.<sup>56</sup> We estimate the MMHg catch of each country and the global potential human MMHg exposure. However, the MMHg content in fish cannot be linked to

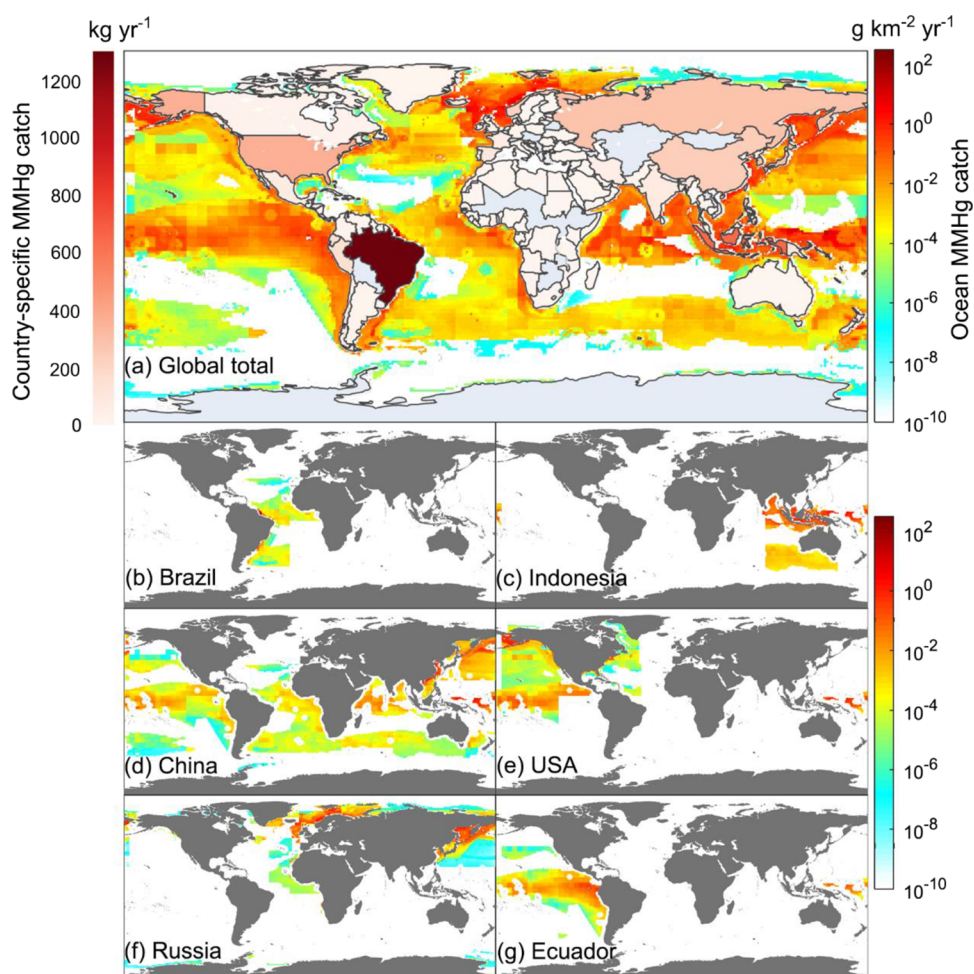


**Figure 7.** MMHg catch. (a) Annual MMHg catch of each country [ $\text{kg yr}^{-1}$ ] and spatial pattern of total MMHg catch across the global ocean [ $\text{g km}^{-2} \text{yr}^{-1}$ ]. (b–g) Spatial pattern of MMHg catch of different countries [ $\text{g km}^{-2} \text{yr}^{-1}$ ].

country-specific exposure, yet, as the marine fish trade is not considered in this study. Future work also includes a better tagging of the emissions from individual countries and rivers, by which we can trace the entire path of Hg from emissions to human exposure.

**3.6. Implications.** This study develops a trophic dynamic model for MMHg in global fish food webs by coupling with a state-of-the-art fish ecology model. It reveals the spatial pattern of MMHg in marine fish and identifies medium-sized fish as key species in MMHg trophic dynamics. We found that grazing, regulated by the structures of food webs, is the key process that affects the magnitudes of MMHg content in fish and the degrees of MMHg biomagnification. These findings can be used to infer the impact of global change. Ongoing large-scale environmental changes such as acidification, seawater temperature change, and overfishing have been shown to have a great impact on marine ecosystem and MMHg in marine fish. For example, ocean acidification could enhance the growth of small phytoplankton and promote the MMHg uptake, which might be propagated to upper TLs.<sup>57</sup> In the less productive future ocean, MMHg content in organisms at high TLs could be significantly increased.<sup>21</sup> Overfishing can cause dietary shifts of marine predators, which in turn will influence the bioaccumulation of MMHg.<sup>7,58,59</sup> Additionally, it can indirectly affect human exposure to MMHg through seafood consumption.

Our model reveals unexpected spatial decoupling between MMHg catch and fish catch and finds the largest contributor to MMHg catch. Thus, it can serve as a useful tool to quantify human exposure to MMHg through marine fish consumption and make better guidelines on the human diet. For example, to reduce the risk of exposure to MMHg through marine fish, less frequent consumption of large pelagic fish (e.g., tunas and billfish) and demersal fish (e.g., cod and halibut), especially those from the oceans where fish are highly MMHg contaminated, is recommended. Instead, epipelagic fish, such as sardines and anchovies, are better choices. Coastal fisheries contribute to the majority of human exposure, and rivers are the largest source of mercury to coastal oceans, which deserves a greater concern.<sup>37,51</sup> The model fills a critical gap in the effectiveness evaluation of the Minamata Convention on Mercury by mechanically linking the reduced anthropogenic emissions of mercury (via atmosphere and riverine discharge), marine fish MMHg level, and global fish MMHg catch.

## ■ ASSOCIATED CONTENT

### SI Supporting Information

The Supporting Information is available free of charge at <https://pubs.acs.org/doi/10.1021/acs.est.3c01299>.

Fish-Hg-seawater data (XLSX)

Model parameterization (Tables S1–S3); spatial pattern of MMHg concentrations in marine zooplankton and



fish, fish biomass, and maximum TL (Figures S1–S3); grazing fluxes in the marine fish food webs (Figure S4); and annual fish catch (Figure S5) (PDF)

## AUTHOR INFORMATION

### Corresponding Author

**Yanxu Zhang** – School of Atmospheric Sciences and Frontiers Science Center for Critical Earth Material Cycling, Nanjing University, Nanjing, Jiangsu 210023, China; [orcid.org/0000-0001-7770-3466](https://orcid.org/0000-0001-7770-3466); Email: [zhangyx@nju.edu.cn](mailto:zhangyx@nju.edu.cn)

### Author

**Peipei Wu** – School of Atmospheric Sciences, Nanjing University, Nanjing, Jiangsu 210023, China

Complete contact information is available at:  
<https://pubs.acs.org/10.1021/acs.est.3c01299>

### Notes

The authors declare no competing financial interest.

## ACKNOWLEDGMENTS

We greatly appreciate the help from Dr. P. Daniël van Denderen on running the FEISTY model. We thank Zhengcheng Song, Tengfei Yuan, Peng Zhang, Dong Peng, Shibao Wang, Yujuan Wang, Siyu Zhu, Ruirong Chang, Qiaotong Pang, Yiming Fu, Mao Mao, and Shaojian Huang for processing Fishbase data and Dr. Tao Huang for data visualization. This study is supported by the National Natural Science Foundation of China (42177349), the Fundamental Research Funds for the Central Universities (Grant nos. 14380188 and 14380168), the Frontiers Science Center for Critical Earth Material Cycling, and the Collaborative Innovation Center of Climate Change, Jiangsu Province.

## REFERENCES

- (1) Budnik, L. T.; Casteleyn, L. Mercury pollution in modern times and its socio-medical consequences. *Sci. Total Environ.* **2019**, *654*, 720–734.
- (2) Axelrad, D. A.; Bellinger, D. C.; Ryan, L. M.; Woodruff, T. J. Dose-response relationship of prenatal mercury exposure and IQ: An integrative analysis of epidemiologic data. *Environ. Health Perspect.* **2007**, *115*, 609–615.
- (3) Sakamoto, M.; Tatsuta, N.; Izumo, K.; Phan, P. T.; Vu, L. D.; Yamamoto, M.; Nakamura, M.; Nakai, K.; Murata, K. Health impacts and biomarkers of prenatal exposure to methylmercury: Lessons from Minamata, Japan. *Toxics* **2018**, *6*, 45.
- (4) Zhang, Y.; Song, Z.; Huang, S.; Zhang, P.; Peng, Y.; Wu, P.; Gu, J.; Dutkiewicz, S.; Zhang, H.; Wu, S.; Wang, F.; Chen, L.; Wang, S.; Li, P. Global Health Effects of Future Atmospheric Mercury Emissions. *Nat. Commun.* **2021**, *12*, 3035.
- (5) Sunderland, E. M.; Li, M.; Bullard, K. Decadal changes in the edible supply of seafood and methylmercury exposure in the United States. *Environ. Health Perspect.* **2018**, *126*, 029003–029003.
- (6) Visnjevec, A. M.; Kocman, D.; Horvat, M. Human mercury exposure and effects in Europe. *Environ. Toxicol. Chem.* **2014**, *33*, 1259–1270.
- (7) Schartup, A. T.; Thackray, C. P.; Qureshi, A.; Dassuncao, C.; Gillespie, K.; Hanke, A.; Sunderland, E. M. Climate change and overfishing increase neurotoxicant in marine predators. *Nature* **2019**, *572*, 648–650.
- (8) Zhang, Y.; Soerensen, A. L.; Schartup, A. T.; Sunderland, E. M. A global model for methylmercury formation and uptake at the base of marine food web. *Global Biogeochem. Cycles* **2020**, *34*, No. e2019GB006348.
- (9) Li, M.-L.; Gillies, E. J.; Briner, R.; Hoover, C. A.; Sora, K. J.; Loseto, L. L.; Walters, W. J.; Cheung, W. W. L.; Giang, A. Investigating the dynamics of methylmercury bioaccumulation in the Beaufort Sea shelf food web: a modeling perspective. *Environ. Sci.: Processes Impacts* **2022**, *24*, 1010–1025.
- (10) Jinadasa, B. K. K.; Jayasinghe, G. D. T. M.; Pohl, P.; Fowler, S. W. Mitigating the impact of mercury contaminants in fish and other seafood—A review. *Mar. Pollut. Bull.* **2021**, *171*, No. 112710.
- (11) Gworek, B.; Bemowska-Kalabun, O.; Kijeńska, M.; Wrzosek-Jakubowska, J. Mercury in marine and oceanic waters—a review. *Water, Air, Soil Pollut.* **2016**, *227*, 371.
- (12) Tseng, C.-M.; Ang, S.-J.; Chen, Y.-S.; Shiao, J.-C.; Lamborg, C. H.; He, X.; Reinfelder, J. R. Bluefin tuna reveal global patterns of mercury pollution and bioavailability in the world's oceans. *Proc. Natl. Acad. Sci. U. S. A.* **2021**, *118*, No. e2111205118.
- (13) Yoshino, K.; Mori, K.; Kanaya, G.; Kojima, S.; Henmi, Y.; Matsuyama, A.; Yamamoto, M. Food sources are more important than biomagnification on mercury bioaccumulation in marine fishes. *Environ. Pollut.* **2020**, *262*, No. 113982.
- (14) Chen, C.; Amirbahman, A.; Fisher, N.; Harding, G.; Lamborg, C.; Nacci, D.; Taylor, D. Methylmercury in marine ecosystems: spatial patterns and processes of production, bioaccumulation, and biomagnification. *EcoHealth* **2008**, *5*, 399–408.
- (15) Sevillano-Morales, J. S.; Cejudo-Gómez, M.; Ramírez-Ojeda, A. M.; Martos, F. C.; Moreno-Rojas, R. Risk profile of methylmercury in seafood. *Curr. Opin. Food Sci.* **2015**, *6*, 53–60.
- (16) Simoneau, M.; Lucotte, M.; Garceau, S.; Laliberte, D. Fish growth rates modulate mercury concentrations in walleye (*Sander vitreus*) from eastern Canadian lakes. *Environ. Res.* **2005**, *98*, 73–82.
- (17) Trudel, M.; Rasmussen, J. B. Modeling the elimination of mercury by fish. *Environ. Sci. Technol.* **1997**, *31*, 1716–1722.
- (18) Lavoie, R. A.; Jardine, T. D.; Chumchal, M. M.; Kidd, K. A.; Campbell, L. M. Biomagnification of mercury in aquatic food webs: A worldwide meta-analysis. *Environ. Sci. Technol.* **2013**, *47*, 13385–13394.
- (19) Al-Reasi, H. A.; Ababneh, F. A.; Lean, D. R. Evaluating mercury biomagnification in fish from a tropical marine environment using stable isotopes ( $\delta^{13}\text{C}$  AND  $\delta^{15}\text{N}$ ). *Environ. Toxicol. Chem.* **2010**, *26*, 1572–1581.
- (20) Karimi, R.; Chen, C. Y.; Pickhardt, P. C.; Fisher, N. S.; Folt, C. L. Stoichiometric controls of mercury dilution by growth. *Proc. Natl. Acad. Sci. U. S. A.* **2007**, *104*, 7477–7482.
- (21) Wu, P.; Dutkiewicz, S.; Monier, E.; Zhang, Y. Bottom-heavy trophic pyramids impair methylmercury biomagnification in the marine plankton ecosystems. *Environ. Sci. Technol.* **2021**, *55*, 15476–15483.
- (22) Wu, P.; Zakem, E. J.; Dutkiewicz, S.; Zhang, Y. Biomagnification of methylmercury in a marine plankton ecosystem. *Environ. Sci. Technol.* **2020**, *54*, 5446–5455.
- (23) van Denderen, P. D.; Petrik, C. M.; Stock, C. A.; Andersen, K. H. Emergent global biogeography of marine fish food webs. *Glob. Ecol. Biogeogr.* **2021**, *30*, 1822–1834.
- (24) Petrik, C. M.; Stock, C. A.; Andersen, K. H.; van Denderen, P. D.; Watson, J. R. Bottom-up drivers of global patterns of demersal, forage, and pelagic fishes. *Prog. Oceanogr.* **2019**, *176*, No. 102124.
- (25) Watson, R. A. A database of global marine commercial, small-scale, illegal and unreported fisheries catch 1950–2014. *Sci. Data* **2017**, *4*, 170039.
- (26) Bowman, K. L.; Hammerschmidt, C. R.; Lamborg, C. H.; Swarr, G. Mercury in the North Atlantic Ocean: The U.S. GEOTRACES zonal and meridional sections. *Deep Sea Res. Part II: Top. Stud. Oceanogr.* **2015**, *116*, 251–261.
- (27) Bowman, K. L.; Hammerschmidt, C. R.; Lamborg, C. H.; Swarr, G. J.; Agather, A. M. Distribution of mercury species across a zonal section of the eastern tropical South Pacific Ocean (U.S. GEOTRACES GP16). *Mar. Chem.* **2016**, *186*, 156–166.
- (28) Gosnell, K. J.; Mason, R. P. Mercury and methylmercury incidence and bioaccumulation in plankton from the central Pacific Ocean. *Mar. Chem.* **2015**, *177*, 772–780.

- (29) Hirota, R.; Fukuda, Y.; Chiba, J.; Tajima, S.; Fujiki, M. Mercury content of copepods (*Crustacea*) collected from the Antarctic Sea. *Polar Res. Repos.* **1989**, *2*, 65–70.
- (30) Barnes, C.; Maxwell, D.; Reuman, D. C.; Jennings, S. Global patterns in predator–prey size relationships reveal size dependency of trophic transfer efficiency. *Ecology* **2010**, *91*, 222–232.
- (31) Chassot, E.; Bonhommeau, S.; Dulvy, N. K.; Mélin, F.; Watson, R.; Gascuel, D.; Pape, O. L. Global marine primary production constrains fisheries catches. *Ecol. Lett.* **2010**, *13*, 495–505.
- (32) Palomares, M.-L. D.; Pauly, D., Chapter 32 - Coastal Fisheries: The Past, Present, and Possible Futures. In *Coasts and Estuarine*, Wolanski, E.; Day, J. W.; Elliott, M.; Ramachandran, R., Eds.; Elsevier: 2019; 569–576.
- (33) Sogn-Grundtvåg, G.; Hermansen, Ø. Quality-enhancing fishing in the coastal fishery for Atlantic cod in Norway. *Mar. Policy* **2022**, *143*, No. 105191.
- (34) Zhang, Y.; Jacob, D. J.; Dutkiewicz, S.; Amos, H. M.; Long, M. S.; Sunderland, E. M. Biogeochemical drivers of the fate of riverine mercury discharged to the global and Arctic oceans. *Global Biogeochem. Cycles* **2015**, *29*, 854–864.
- (35) Pauly, D.; Trites, A. W.; Capuli, E.; Christensen, V. Diet composition and trophic levels of marine mammals. *ICES J. Mar. Sci.* **1998**, *55*, 467–481.
- (36) Borga, K.; Kidd, K. A.; Muir, D. C. G.; Berglund, O.; Conder, J. M.; Gobas, F. A. P. C.; Kucklick, J. R.; Malm, O.; Powell, D. E. Trophic magnification factors: Considerations of ecology, ecosystems, and study design. *Integr. Environ. Assess. Manag.* **2012**, *8*, 64–84.
- (37) Liu, M.; Zhang, Q.; Maavara, T.; Liu, S.; Wang, X.; Raymond, P. A. Rivers as the largest source of mercury to coastal oceans worldwide. *Nat. Geosci.* **2021**, *14*, 672–677.
- (38) Galvao, P.; Sus, B.; Lailson-Brito, J.; Azevedo, A.; Malm, O.; Bisi, T. An upwelling area as a hot spot for mercury biomonitoring in a climate change scenario: A case study with large demersal fishes from Southeast Atlantic (SE-Brazil). *Chemosphere* **2021**, *269*, No. 128718.
- (39) Bonsignore, M.; Manta, D. S.; Oliveri, E.; Sprovieri, M.; Basilone, G.; Bonanno, A.; Falco, F.; Traina, A.; Mazzola, S. Mercury in fishes from Augusta Bay (southern Italy): Risk assessment and health implication. *Food Chem. Toxicol.* **2013**, *56*, 184–194.
- (40) Jędruch, A.; Falkowska, L.; Saniewska, D.; Grajewska, A.; Beldowska, M.; Meissner, W.; Kalisińska, E.; Duzinkiewicz, K.; Pacyna, J. M. Mercury in the Polish part of the Baltic Sea: A response to decreased atmospheric deposition and changing environment. *Mar. Pollut. Bull.* **2023**, *186*, No. 114426.
- (41) Jonathan, M. P.; Auriolles-Gamboa, D.; Villegas, L. E. C.; Bohórquez-Herrera, J.; Hernández-Camacho, C. J.; Sujitha, S. B. Metal concentrations in demersal fish species from Santa Maria Bay, Baja California Sur, Mexico (Pacific coast). *Mar. Pollut. Bull.* **2015**, *99*, 356–361.
- (42) Romero-Romero, S.; García-Ordiales, E.; Roqueñí, N.; Acuña, J. L. Increase in mercury and methylmercury levels with depth in a fish assemblage. *Chemosphere* **2022**, *292*, No. 133445.
- (43) Karimi, R.; Chen, C. Y.; Folt, C. L. Comparing nearshore benthic and pelagic prey as mercury sources to lake fish: the importance of prey quality and mercury content. *Sci. Total Environ.* **2016**, *565*, 211–221.
- (44) Ward, D. M.; Nislow, K. H.; Chen, C. Y.; Folt, C. L. Reduced trace element concentrations in fast-growing juvenile Atlantic salmon in natural streams. *Environ. Sci. Technol.* **2010**, *44*, 3245–3251.
- (45) van der Velden, S.; Evans, M. S.; Dempson, J. B.; Muir, D. C. G.; Power, M. Comparative analysis of total mercury concentrations in anadromous and non-anadromous Arctic charr (*Salvelinus alpinus*) from eastern Canada. *Sci. Total Environ.* **2013**, *447*, 438–449.
- (46) Chételat, J.; Shao, Y.; Richardson, M. C.; MacMillan, G. A.; Amyot, M.; Drevnick, P. E.; Gill, H.; Köcke, G.; Muir, D. C. G. Diet influences on growth and mercury concentrations of two salmonid species from lakes in the eastern Canadian Arctic. *Environ. Pollut.* **2021**, *268*, No. 115820.
- (47) Vallina, S. M.; Follows, M. J.; Dutkiewicz, S.; Montoya, J. M.; Cermeno, P.; Loreau, M. Global relationship between phytoplankton diversity and productivity in the ocean. *Nat. Commun.* **2014**, *5*, 4299.
- (48) Gasol, J. M.; del Giorgio, P. A.; Duarte, C. M. Biomass distribution in marine planktonic communities. *Limnol. Oceanogr.* **1997**, *42*, 1353–1363.
- (49) Hatton, I. A.; McCann, K. S.; Fryxell, J. M.; Davies, T. J.; Smerlak, M.; Sinclair, A. R. E.; Loreau, M. The predator-prey power law: Biomass scaling across terrestrial and aquatic biomes. *Science* **2015**, *349*, No. aac6284.
- (50) Cresson, P.; Chauvelon, T.; Bustamante, P.; Bănar, D.; Baudrier, J.; Loc'h, F. L.; Mauffret, A.; Mialet, B.; Spitz, J.; Wessel, N.; Briand, M. J.; Denamiel, M.; Doray, M.; Guillou, G.; Jadaud, A.; Lazard, C.; Prieur, S.; Rouquette, M.; Saraux, C.; Serre, S.; Timmerman, C.-A.; Verin, Y.; Harmelin-Vivien, M. Primary production and depth drive different trophic structure and functioning of fish assemblages in French marine ecosystems. *Prog. Oceanogr.* **2020**, *186*, No. 102343.
- (51) Lavoie, R. A.; Bouffard, A.; Maranger, R.; Amyot, M. Mercury transport and human exposure from global marine fisheries. *Sci. Rep.* **2018**, *8*, 6705.
- (52) Bastos, W. R.; Dórea, J. G.; Bernardi, J. V. E.; Lauthartte, L. C.; Mussu, M. H.; Lacerda, L. D.; Malm, O. Mercury in fish of the Madeira river (temporal and spatial assessment), Brazilian Amazon. *Environ. Res.* **2015**, *140*, 191–197.
- (53) Dorea, J. G.; Moreira, M. B.; East, G.; Barbosa, A. C. Selenium and mercury concentrations in some fish species of the Madeira River, Amazon Basin, Brazil. *Biol. Trace Elem. Res.* **1998**, *65*, 211–220.
- (54) Lacerda, L. D.; Goyanna, F.; Bezerra, M. F.; Silva, G. B. Mercury concentrations in tuna (*Thunnus albacares* and *Thunnus obesus*) from the Brazilian Equatorial Atlantic Ocean. *Bull. Environ. Contam. Toxicol.* **2017**, *98*, 149–155.
- (55) Vieira, H. C.; Osten, J. R.-V.; Soares, A. M. V. M.; Morgado, F.; Abreu, S. N. Mercury bioaccumulation in the long-fin squid *Loligo forbesi* near the Mid-Atlantic Ridge: Implications to human exposure. *Ecotoxicol. Environ. Saf.* **2020**, *203*, No. 110957.
- (56) Seco, J.; Xavier, J. C.; Brierley, A. S.; Bustamante, P.; Coelho, J. P.; Gregory, S.; Fielding, S.; Pardal, M. A.; Pereira, B.; Stowasser, G.; Tarling, G. A.; Pereira, E. Mercury levels in Southern Ocean squid: Variability over the last decade. *Chemosphere* **2020**, *239*, No. 124785.
- (57) Zhang, Y.; Dutkiewicz, S.; Sunderland, E. M. Impacts of climate change on methylmercury formation and bioaccumulation in the 21st century ocean. *One Earth* **2021**, *4*, 279–288.
- (58) Zhang, H.; Wang, W.; Lin, C.; Feng, X.; Shi, J.; Jiang, G.; Larssen, T. Decreasing mercury levels in consumer fish over the three decades of increasing mercury emissions in China. *Eco-Environ. Health* **2022**, *1*, 46–52.
- (59) Pan, K.; Chan, H.; Tam, Y. K.; Wang, W.-X. Low mercury levels in marine fish from estuarine and coastal environments in southern China. *Environ. Pollut.* **2014**, *185*, 250–257.